J Neuroimmune Pharmacol (2016) 11:572–583
DOI 10.1007/s11481-016-9654-0

ORIGINAL ARTICLE

Brain Invasion by CD4$^+$ T Cells Infected with a Transmitted/Founder HIV-1$_{BJZS7}$ During Acute Stage in Humanized Mice

Xilin Wu[1] · Li Liu[1,2] · Ka-wai Cheung[1] · Hui Wang[2] · Xiaofan Lu[3] · Allen Ka Loon Cheung[1] · Wan Liu[1] · Xiuyan Huang[1] · Yanlei Li[1] · Zhiwei W. Chen[1,4] · Samantha M. Y. Chen[1] · Tong Zhang[3] · Hao Wu[3] · Zhiwei Chen[1,2]

Received: 12 November 2015 / Accepted: 25 January 2016 / Published online: 2 February 2016

Abstract Human immunodeficiency virus (HIV)-associated neurocognitive disorder (HAND) is one of the common causes of cognitive dysfunction and morbidity among infected patients. However, to date, it remains unknown if a transmitted/founder (T/F) HIV-1 leads to neurological disorders during acute phase of infection. Since it is impossible to answer this question in humans, we studied NOD.Cg-Prkdc scid Il2rgtm1Wjl/SzJ mice (NSG) reconstituted with human PBMC (NSG-HuPBL), followed by the peritoneal challenge with the chronic HIV-1$_{JR-FL}$ and the T/F HIV-1$_{BJZS7}$, respectively. By measuring viral load, P24 antigenemia and P24$^+$ cells in peripheral blood and various tissue compartments, we found that systemic infections were rapidly established in NSG-HuPBL mice by both HIV-1 strains. Although comparable peripheral viral loads were detected during acute infection, the T/F virus appeared to cause less CD4$^+$ T cell loss and less numbers of infected cells in different organs and tissue compartments. Both viruses, however, invaded brains with P24$^+$/CD3$^+$ T cells detected primarily in meninges, cerebral cortex and perivascular areas. Critically, brain infections with HIV-1$_{JR-FL}$ but not with HIV-1$_{BJZS7}$ resulted in damaged neurons together with activated microgliosis and astrocytosis as determined by significantly increased numbers of Iba1$^+$ microglial cells and GFAP$^+$ astrocytes, respectively. The increased Iba1$^+$ microglia was correlated positively with levels of P24 antigenemia and negatively with numbers of NeuN$^+$ neurons in brains of infected animals. Our findings, therefore, indicate the establishment of two useful NSG-HuPBL models, which may facilitate future investigation of mechanisms underlying HIV-1-induced microgliosis and astrocytosis.

Keywords HIV-1 · NSG · HAND · Acute infection · Transmitted/founder

✉ Zhiwei Chen
zchenai@hku.hk

[1] AIDS Institute and Department of Microbiology, Research Centre for Infection and Immunity, Li Ka Shing Faculty of Medicine, The University of Hong Kong, L5-45, 21 Sassoon Road, Pokfulam, Hong Kong SAR, People's Republic of China

[2] HKU-AIDS Institute Shenzhen Research Laboratory and AIDS Clinical Research Laboratory, Guangdong Key Lab of Emerging Infectious Diseases and Shenzhen Key Lab of Infection and Immunity, Shenzhen Third People's Hospital, Guangdong Medical College, Shenzhen 518112, People's Republic of China

[3] Beijing You'an Hospital, Capital Medical University, Beijing, People's Republic of China

[4] Fuzhou Center for Disease Control and Prevention, Fujian Medical University, Fuzhou, People's Republic of China

Introduction

According to UNAIDS, there are estimated 36.9 million of people living with human immunodeficiency virus type one (HIV-1) in the world by the end of 2014. HIV-1-infected individuals commonly develop neurological disorders, namely HIV-1-associated neurocognitive disorder (HAND). Accordingly, HAND ranges from subtle to substantial neurocognitive impairments including HIV-1-associated dementia (HAD) and milder forms known as asymptomatic neurocognitive impairment (ANI) as well as mild neurocognitive disorder (MND)(Rumbaugh and Tyor 2015). Currently, the mortality of HAND complications and opportunistic infections remains high among untreated HIV-1-infected individuals particularly with those unaware of their

infection status (Maartens et al. 2014a; Matinella et al. 2015). Furthermore, despite antiretroviral treatment (ART), which reduces HIV-1 disease progression, mortality and transmission, ANI and MND are still highly prevalent (Matinella et al. 2015; Watkins and Treisman 2015). A substantial proportion of patients with suppressed viral infection on optimal ART have developed ANI and MND, suggesting the persistence of neurological abnormalities despite treatment and projected long-term survival. It is, therefore, necessary to investigate deeply the mechanism underlying HAND during HIV-1 infection.

Since it is difficult to obtain specimens of central nervous system (CNS) in humans, animal models have been employed for the investigation of HIV-1 encephalitis (Harbison et al. 2014; Persidsky et al. 1996; Zhuang et al. 2014). Intracranial injection of HIV-infected human monocyte-derived macrophages (MDM) in SCID mice has resulted in neurological disorders similar to humans such as multinucleated giant cells (MGC), astrogliosis, myelin pallor, and predominant neuronal dropout (Budka et al. 1991; Persidsky et al. 1996; Tyor et al. 1993). HAND diseases have been documented with rhesus macaques experimentally infected with simian-human immunodeficiency virus (SHIV) (Harbison et al. 2014; Zhuang et al. 2014). Moreover, the engraftment of functional human immune system was achieved in immune deficient mice including NOD-scid IL2R γ^{null} (NSG)(Watanabe et al. 2007), BALB/c-Rag2$^{-/-}\gamma c^{-/-}$ (BRG)(Baenziger et al. 2006), and NOD/scid strains (Kumar et al. 2008). These rodent models have been used in studying HIV-1 pathogenesis and therapeutic interventions, which also offer a convenient tool to explore neuropathogenesis of HAND (Gorantla et al. 2010; Gorantla et al. 2012). To date, however, it remains unknown if the transmitted/founder (T/F) HIV-1 leads to neuropathogenesis during the acute phase of infection.

In recent years, many studies have focused on acute events of T/F infection, which provided critical information about HIV-1 transmission bottlenecks and how these bottlenecks might affect HIV-1 prevention strategies (Joseph et al. 2015; Keele et al. 2008). It has been well documented that approximately 80 % of heterosexually transmitted infections are established from a single T/F HIV-1 variant (Joseph et al. 2015; Keele et al. 2008). Moreover, the early neuronal injury has been found in some patients with primary HIV-1 infection probably through mechanisms involving CNS inflammation (Peluso et al. 2013). Other studies also demonstrated that CSF viral load was detectable as early as 8 days after HIV-1 exposure among some individuals whose CNS inflammation was apparent by CSF analysis and magnetic resonance spectroscopy (MRS) (Sailasuta et al. 2012; Valcour et al. 2012). We, therefore, aimed to compare the CNS injury between a newly isolated T/F HIV-1 strain, namely HIV-1_{BJZS7}, and the well-known chronic isolate HIV-$1_{JR\text{-}FL}$ using NSG mice reconstituted with human PBMC (NSG-HuPBL).

Materials and Methods

Virus

HIV-$1_{JR\text{-}FL}$, a chronic isolate, was propagated in primary human peripheral blood mononuclear cells (PBMCs) as described previously (Chen et al. 1997). HIV-1_{BJZS7} was newly isolated in our bio-safety level 3 laboratory (BSL-3) from a 20 years old man in an acute cohort of MSM infections in Beijing (Chen et al. 2015). We obtained the written consent from all individuals who participated in the cohort study, which was approved by the ethics committee of You'an hospital. Fiebig stages were based on the measurement of viral load and sero-positivity. Based on monthly follow-ups for HIV-1 infection, the blood sample was collected about 45 days post infection with weak seroconversion. HIV-1_{BJZS7}, therefore, fits Fiebig stage V as a newly isolated live T/F strain. The viral stock was also propagated in primary human PBMCs.

Animals

All animal experiments were approved by the Committee on the Use of Live Animals in Teaching and Research at the Laboratory Animal Unit of The University of Hong Kong. Immunodeficient NOD.Cg-Prkdc scid Il2rgtm1Wjl/SzJ (NSG) mice were purchased from the Jackson Laboratory. NSG-HuPBL mice were generated as described previously (Nakata et al. 2005). Briefly, $2x10^7$ PBMCs, which were freshly isolated from healthy blood donors, were injected intraperitoneally (i.p.) (in 0.5 ml RPMI) into each of 4- to 6-week-old NSG mice. PBMC engraftments were tested 21 days after the transplantation by FACS-staining of human $CD45^+$, $CD3^+$, $CD4^+$ and $CD8^+$ cells (Fig.1a).

HIV-1 Challenge Experiment

One day before the HIV-1 challenge, animal blood samples were subjected to ELISA for antibody quantification and to flow cytometry analysis to determine the baseline ratio of CD4/CD8 T-lymphocytes. On the day of viral challenge, mice were injected through i.p. with 10 ng p24, a dose described by others (Balazs et al. 2012; Balazs et al. 2014), of either the chronic HIV-$1_{JR\text{-}FL}$ strain (466 $TCID_{50}$) or the T/F HIV-1_{BJZS7} strain (646 $TCID_{50}$). The $TCID_{50}$ value was determined by infecting TZM-bl cells as previously described (Kang et al. 2012). Infected mice were subjected to weekly blood sampling to determine the cell frequency and CD4/CD8 ratio by flow cytometry and to test the viral load by quantitative RT-PCR (qRT-PCR) in our BSL-3 laboratory.

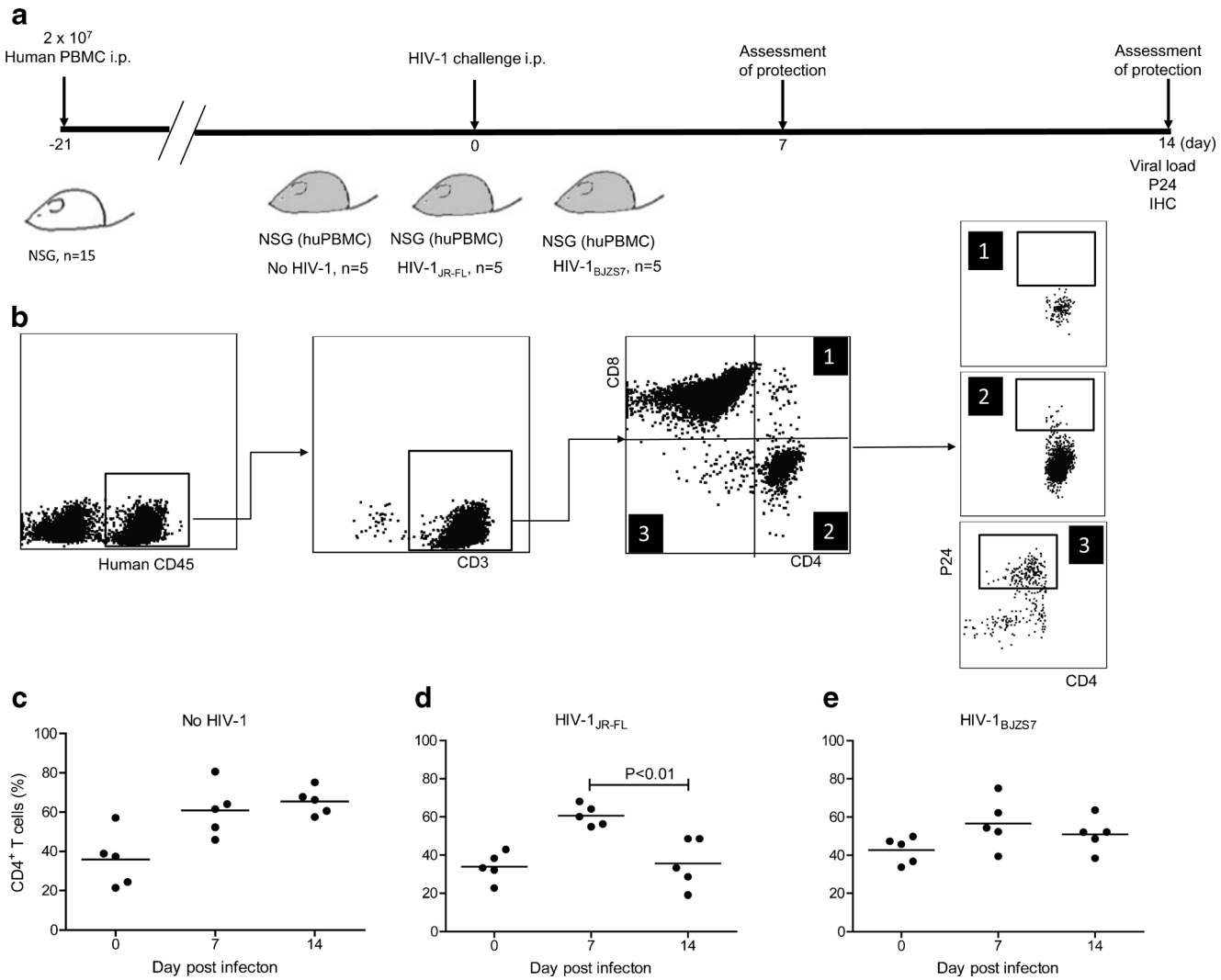

Fig. 1 HIV-1 Infection of NSG-HuPBL mice. **a** Experimental schedule. **b** Flow cytometry analysis of human $CD45^+$ cells, $CD3^+$ T cells and $P24^+$ T cells after infection by the T/F HIV-1_{BJZS7}. **c** The percentage of $CD4^+$ T cells among uninfected NSG-HuPBL mice. **d** The percentage of $CD4^+$ T cells among HIV-1_{JR-FL}-infected NSG-HuPBL mice overtime. **e** The percentage of $CD4^+$ T cells among HIV-1_{BJZS7}-infected NSG-HuPBL mice overtime

Viral Load Test by qRT-PCR

Viral RNA was extracted using the QIAamp viral RNA mini kit (Qiagen) or RNAiso plus (Takara). Each RNA sample was reversely transcribed into cDNA in 20 μl volume with the RT-PCR Prime Script Kit (Takara). 8 μl of cDNA was used in a 20 μl qRT-PCR reaction with the TaqMan Universal PCR Master Mix (Life technologies), a TaqMan probe (5′-FAM − CTCTCTCCTTCTAGCCTC − MGB-3′) and primers designed targeting the P17 gene of HIV-1_{JR-FL} and HIV-1_{BJZS7} (5′-TACTGACGCTCTCGCACC and 3′-TCTCGACGCAGGACTCG). Samples were run in triplicate on an Eppendorf Realplex4 Mastercycler (Eppendorf). The following cycling conditions were used: 1 cycle of 50 °C for 2 min, 1 cycle of 95 °C for 10 min followed by 40 cycles of 95 °C for 15 s and 60 °C for 1 min. Virus load was determined by comparison with a standard curve generated using RNA extracted from a serially diluted reference viral stock. The limit of detection was 500–1000 copies per ml for HIV-1_{JR-FL} and HIV-1_{BJZS7}.

Flow Cytometry

Blood samples were taken from the facial vein of each animal into tubes containing 50 μl anti-coagulant (0.5 M EDTA), which were then centrifuged for 5 min at 1,150 g in a microcentrifuge to separate plasma from cell pellets. Cell pellets were re-suspended in 2 ml of 1× RBC lysis buffer (BD Bioscience) and incubated at 4 °C for at least 10 min to remove red blood cells. After the lysis, samples were pelleted at 1,150 g in a microcentrifuge for 5 min at room temperature, and stained with 100 μl of a cocktail of antibodies containing

2 μl of each anti-human CD3-PE-cy7, anti-human CD4-Percyp-cy5.5, anti-human CD8-PE antibodies, anti-human CD45 APC, and anti-human CD19 Pacific blue (Bio legend). The cell labeling was performed for 60 min at 4 °C. Samples were washed with 1 ml phosphate buffered saline supplemented with 2 % fetal bovine serum (PBS1) and again pelleted at 1, 150 g in a microcentrifuge for 5 min. Pelleted cells were re-suspended in 300 μl of PBS1 and analyzed on flow cytometer (Beckton-Dickinson Aria III). Cells were first gated for human CD45 expression before analyzing other sub-populations (Fig. 1b).

Immunohistochemical Staining of HIV-1 P24$^+$ Cells

At the conclusion of in vivo challenge experiments, tissues were removed from mice and immersed in 10 % neutral buffered formalin for 24 h. After the fixation, tissues were placed in 70 % ethanol until standard paraffin embedding and processing. Tissue sections (4 μm thick) were subjected to immunohistochemical staining for HIV-P24 detection using P24-specific antibody (Ab) Kal-1, with co-staining of rabbit anti-human CD3 (1/100; DakoCytomation). Confocal images were obtained by Carl Zeiss LSM 700 using the ZEN 2012 software.

Immunohistochemistry of Activated Cells in Brain

Brain tissues were derived from perfused mice and processed as previously described (Gorantla et al. 2007). Murine microglia were detected with rabbit polyclonal Abs to human Iba1 (ionizing calcium-binding adaptor molecule 1) (1/500; Wako). Astrocytes were visualized with rabbit anti-mouse GFAP Ab (1/1,000; DakoCytomation). Anti-HIV-1 p24 Abs (1/5; Dako Cytomation) were used to identify HIV-1-infected cells. T cells were identified by staining of rabbit anti-human CD3 Ab (1/100; DakoCytomation). Ab to neuronal nuclei protein (NeuN) (1/100) was used to identify neurons. Primary Abs were visualized with AlexaFluor 488 (green)- Alexa Fluor 568 (red)- and Alexa Fluor 648 (orange)-conjugated secondary Abs (Invitrogen; Molecular Probes). 4_,6_-diamidino-2-phenylindole (DAPI) were used as a nuclear stain. Confocal images were obtained by Carl Zeiss LSM 700 using the ZEN 2012 software.

Statistical Analysis

FACS data was analyzed with the FlowJo 7.6 program. Mean fluorescence intensity (MFI) was scored using the NIH Image J software. Graphs were generated with the GraphPad Prism 5.01 program (GraphPad Software Inc., La Jolla, CA). Two-tailed student t-tests were used for group comparison. *P* value less than 0.05 was considered to be statistically significant. Data are presented as the mean values ± standard error.

Results

Establishment of HIV-1$_{BJZS7}$ Infection in NSG-HuPBL Mice

To determine the proper population of human T cells in NSG-HuPBL mice, we measured human CD45, CD3, CD4 and CD8 cells by flow cytometry three weeks after the engraftment with PBMC (Fig. 1b-e). The proportion of CD45 positive human cells was consistently about 50 % in peripheral blood of humanized mice. By flow cytometry, HIV-1$_{BJZS7}$ infection resulted in two distinct P24$^+$CD4$^+$ and P24$^+$CD4$^-$ T cell populations (Fig. 1b, gate 2 and 3). The latter one was likely derived from a proportion of P24$^+$CD4$^+$ T cells after infection-induced CD4 downregulation (Fig. 1b, gate 3). Using the same methods, we further investigated T cells in three groups of humanized mice including No HIV-1 (Fig. 1c), HIV-1$_{JR-FL}$(Fig. 1d) and HIV-1$_{BJZS7}$ (Fig. 1e). On the day of viral infection (day 0), the proportion of CD4$^+$ T cells reached around 40 % of total human CD3$^+$ T cells in all three groups (Fig. 1c-e). After viral i.p. inoculation, the frequency of CD4$^+$ T cells was significantly lower on day 14 post infection (dpi) than that on 7 dpi among mice infected with HIV-1$_{JR-FL}$ (Fig. 1c-e). Despite the lack of statistical significance, HIV-1$_{BJZS7}$-infected mice showed similar dropout trend of CD4$^+$ T cells on 14 dpi. At the same time, comparable levels of viral loads reached the average values over 10^6 copies per milliliter in plasma of both HIV-1$_{JR-FL}$ and HIV-1$_{BJZS7}$-infected mice (Fig. 2a), together with readily detected plasma P24 antigenemia (Fig. 2b), suggesting active HIV-1 replication during the acute phase of infection. However, HIV-1 P24 antigenemia was less severe among HIV-1$_{BJZS7}$-infected mice than those infected with HIV-1$_{JR-FL}$ but there was no statistical significance for this comparison. Furthermore, besides peripheral viral loads and antigenemia, productive HIV-1 infection was supported by the detection of P24$^+$ T cells by flow cytometry in both PBMC and spleens of all infected animals but not in controls (Fig. 2c-d). These results are consistent with the CD4$^+$ T cell change of acutely infected people (Maartens et al. 2014b). Based on the detection of viral RNA and P24 (Fig. 2a-d), these NSG-HuPBL mice infected with either HIV-1$_{BJZS7}$ or HIV-1$_{JR-FL}$ were characterized as Fiebig stage II in acute phase of infection (McMichael et al. 2010).

Systemic Dissemination of HIV-1$_{BJZS7}$ Infection in NSG-HuPBL Mice

To understand the extent of viral infection and dissemination in NSG-HuPBL mice, specimens of multiple organs and tissues were further stained for the presence and distribution of infected cells on 14 dpi by immunohistochemical (IHC) techniques. Antigen-specific antibodies were used to detect HIV-1 Gag protein P24 (green) and CD3$^+$ T cells (red). In the lymph

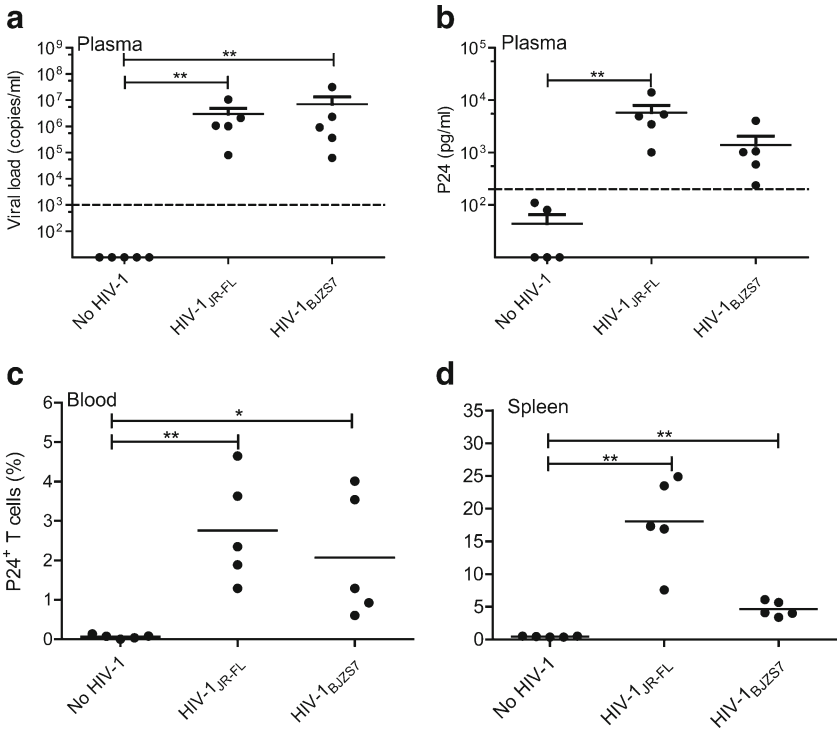

Fig. 2 Characterization of HIV-1-infected NSG-HuPBL mice on 14 dpi. **a** Plasma viral loads were tested among three groups of NSG-HuPBL mice. **d** Plasma P24 antigenemia were determined by ELISA among three groups of animals. **c** The percentage of peripheral $P24^+$ T cells was determined among infected NSG-HuPBL mice by flow cytometry analysis. **d** The percentage of $P24^+$ T cells was determined in spleens of infected NSG-HuPBL mice by flow cytometry analysis. There were no statistical differences between two infection groups. *, $p < 0.05$; **, $p < 0.01$

system, a large number of P24 positive cells were readily found in spleens of mice challenged with both HIV-1_{BJZS7} and HIV-$1_{JR\text{-}FL}$ (Fig 3). Since these infected cells were dual-positive to CD3 (Fig. 3), they were primarily T cells. To less extent, HIV-1_{BJZS7}-infected T cells were found in all organs tested including lung, liver and kidney (Fig. 3). Apparently, HIV-$1_{JR\text{-}FL}$ resulted in more severe lung infections with a larger number of P24 positive T cells as compared with HIV-1_{BJZS7}. In the mucosal digestive system, P24 positive T cells were detected in stomachs, large intestines and small intestines of all HIV-1_{BJZS7}- and HIV-$1_{JR\text{-}FL}$-infected mice (Fig. 4). A larger number of T cells that were recruited to the submucosal areas of lamina propria throughout the stomach, small intestines and large intestines were infected by HIV-$1_{JR\text{-}FL}$ than by HIV-1_{BJZS7}. Collectively, the number of P24 positive T cells was relatively lower in HIV-1_{BJZS7} group as compared to HIV-$1_{JR\text{-}FL}$ group in multiple tissue compartments. Nevertheless, the T/F HIV-1_{BJZS7} was able to establish systemic infection in NSG-HuPBL mice similar to that of HIV-$1_{JR\text{-}FL}$.

Entry of HIV-1_{BJZS7} in Brains of NSG-HuPBL Mice

To understand if HIV-1_{BJZS7} would enter brains of infected mice during the acute phase of infection, we measured viral load and analyzed cells in brain tissue sections for the expression of P24 in *green* and $CD3^+$ T cells in *red* as described above. Consistently, P24 positive T cells were found in meninges and cortex of mice infected with both HIV-1_{BJZS7} and HIV-$1_{JR\text{-}FL}$ (Fig. 5a). In HIV-1_{BJZS7}-infected mice, P24 stained were brighter but were still overlapped with CD3 expression in both meninges and perivascular areas in cortex, suggesting the T cell phenotype of these infected cells. It's clearly shown that some HIV-1_{BJZS7}-infected T cells could enter the cerebral cortex similar to HIV-$1_{JR\text{-}FL}$ infection. Moreover, brain homogenates contained high copy numbers of viral RNA in all infected mice by Q-PCR (Fig. 5b) and measurable levels of P24 protein in most animals by ELISA, respectively (Fig. 5c). Similar to what was found in plasma (Fig. 2c-d), there were relatively lower levels of P24 protein in brain homogenates of HIV-1_{BJZS7}-infected mice than those of HIV-$1_{JR\text{-}FL}$-infected. Taken together, similar to HIV-$1_{JR\text{-}FL}$, HIV-1_{BJZS7} was able to invade the central nervous system likely via infected CD4 T cells at the Fiebig stage II of acute infection.

Neuropathogenesis of HIV-1_{BJZS7} Infection in Brains of NSG-HuPBL Mice

To further understand the neuropathogenesis of HIV-1_{BJZS7} infection, we measured the level of cell activation makers in the brains of infected mice. Infection-induced neuropathogenesis was assessed by the expression of Iba-1 and GFAP as biomarkers of activated microglia and activated astrocytes, respectively (Gorantla et al. 2010). While HIV-1_{BJZS7}-infected mice presented slightly increased levels of Iba1 and GFAP expression as compared with uninfected mice, significantly elevated microglia activation and astrocytes activation were observed in

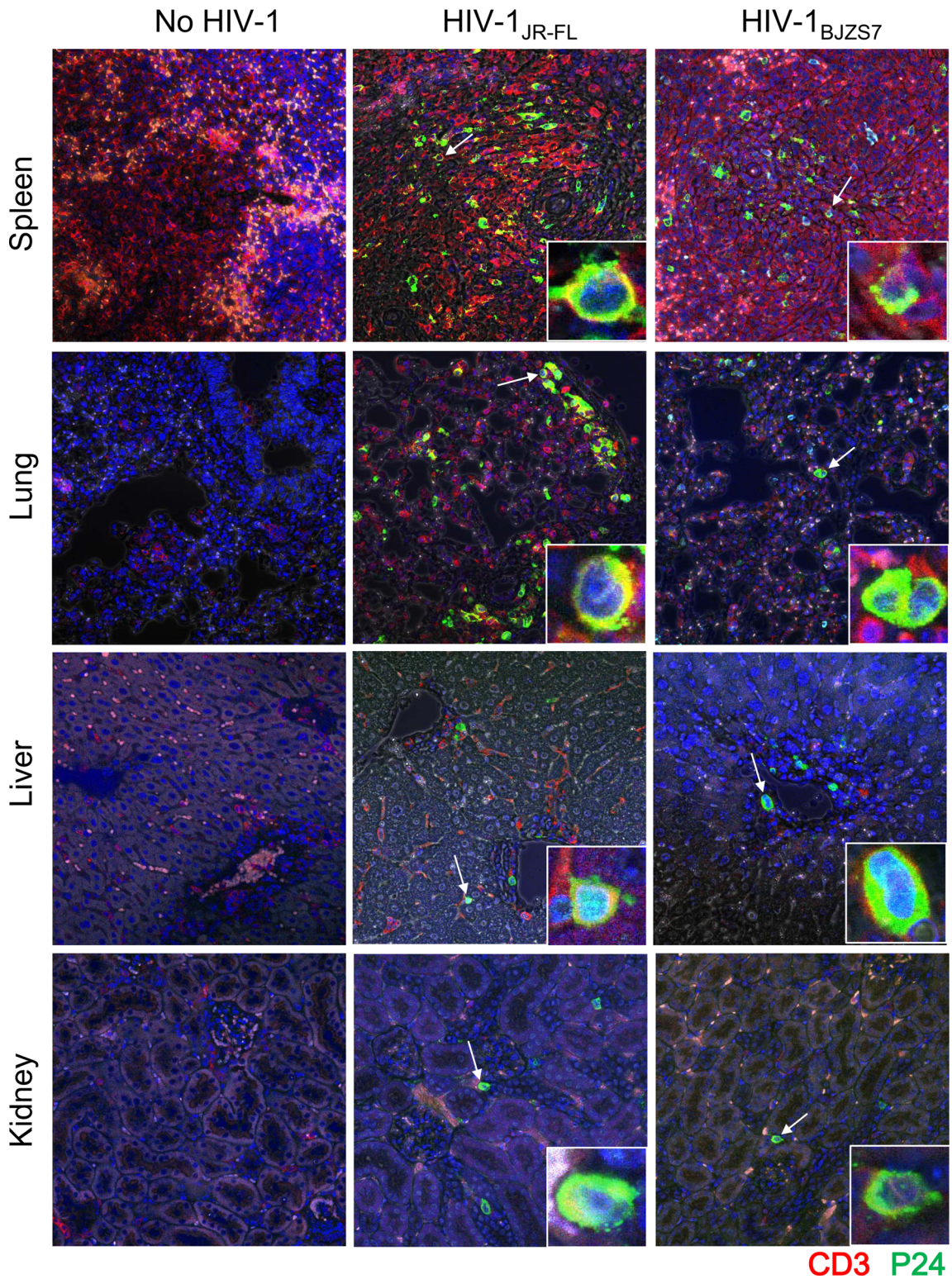

Fig. 3 Systemic distribution of P24^{+} T cells among infected NSG-HuPBL mice by IHC on 14 dpi. Representative tissue sections were analyzed by antibodies specific to HIV-1 P24 in *green* and to human CD3 in *red* among three groups of mice. These tissue sections were derived from spleen, lung, liver and kidney of NSG-HuPBL mice tested. The insets are enlarged images of individual cells pointed by corresponding *arrows*

mice infected by HIV-1_{JR-FL}, suggesting robust microgliosis and astrocytosis (Fig. 6a-b). Since microgliosis and astrocytosis are associated with neuron damage during HIV-1-infection (Liu et al. 2009; Minagar et al. 2002), we further measured the

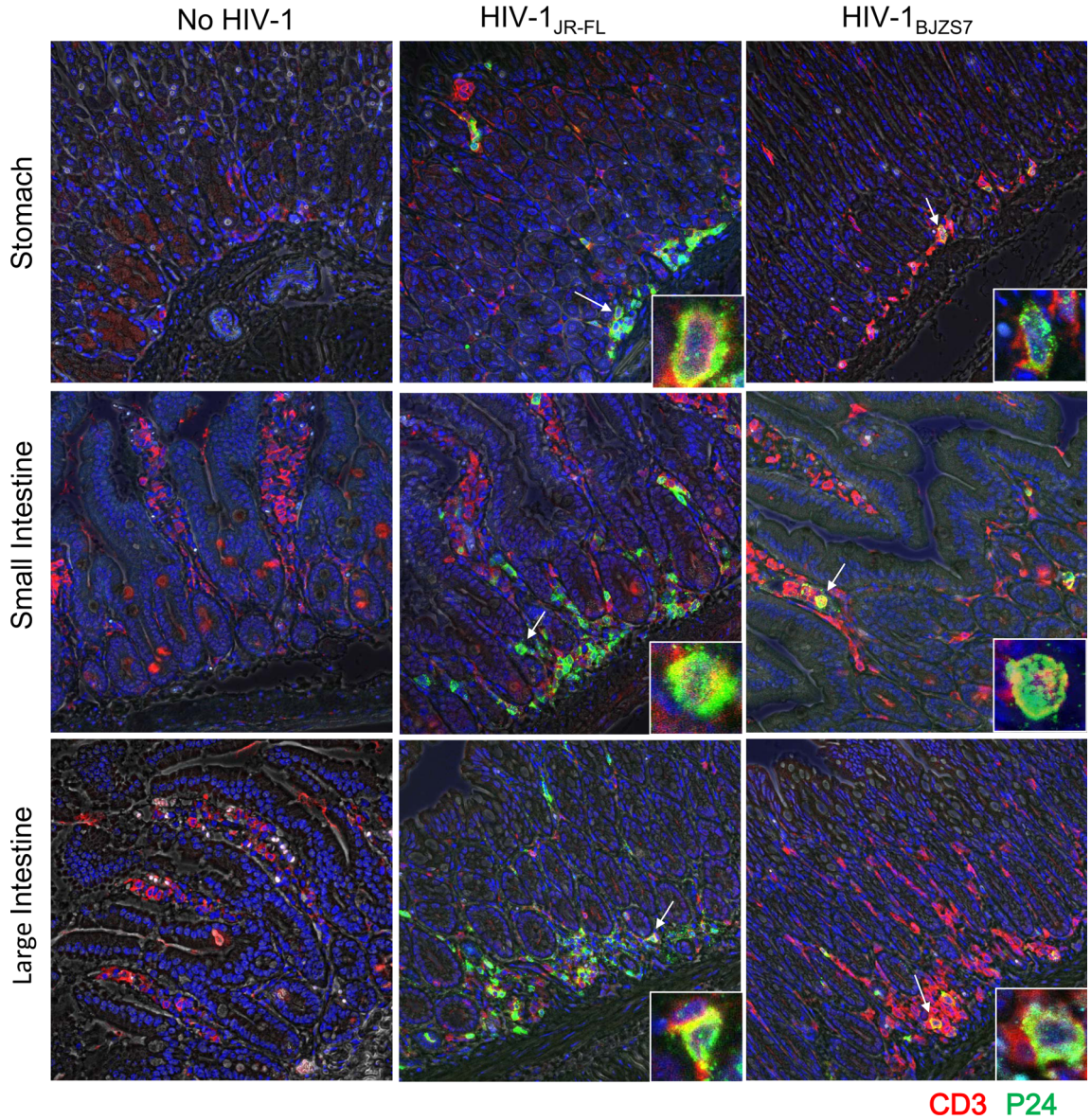

Fig. 4 Distribution of $P24^+$ T cells in mucosal tissues of infected NSG-HuPBL mice by IHC on 14 dpi. Representative tissue sections were analyzed by antibodies specific to HIV-1 P24 in *green* and to human CD3 in r*ed* among three groups of mice. These tissue sections were derived from stomach, small intestine and large intestine of NSG-HuPBL mice tested. The insets are enlarged images of individual cells pointed by corresponding *arrows*

neuronal density in brains of infected animals by staining NeuN, one of the major biomarkers of neuron cells. Consistently, severe neuronal dropout was found mainly in HIV-1_{JR-FL}-infected mice (Fig. 6a-b). In contrast, HIV-1_{BJZS7}-infected mice exhibited insignificant reduction in the number of NeuN-expressing neurons as compared with uninfected control mice. Morphologically, HIV-1_{JR-FL}-infected mice displayed shrunken and likely degenerated neurons, which were not found in HIV-1_{BJZS7}-infected mice. These data likely indicated some differences in neuropathogenesis between chronic HIV-1_{JR-FL} and the T/F HIV-$1_{BJZS7.}$ Interestingly, infected cells were rarely found in areas of neuron damage. There were neither resident microglial cells nor astrocytes found to be P24 positive. Further analysis showed that the level of P24 antigenemia but not viral load was positively correlated with Iba-1 activation, which was further negatively correlated with the number of neurons (Fig. 6c). Excluding control mice (No HIV-1) gave similar correlation results during the analysis. However, there was no significant correlation found for GFAP levels perhaps due to rapid over-activation of astrocytes.

Discussion

In this study, we have used an NSG-HuPBL mouse model to investigate the acute infection of a newly isolated T/F HIV-

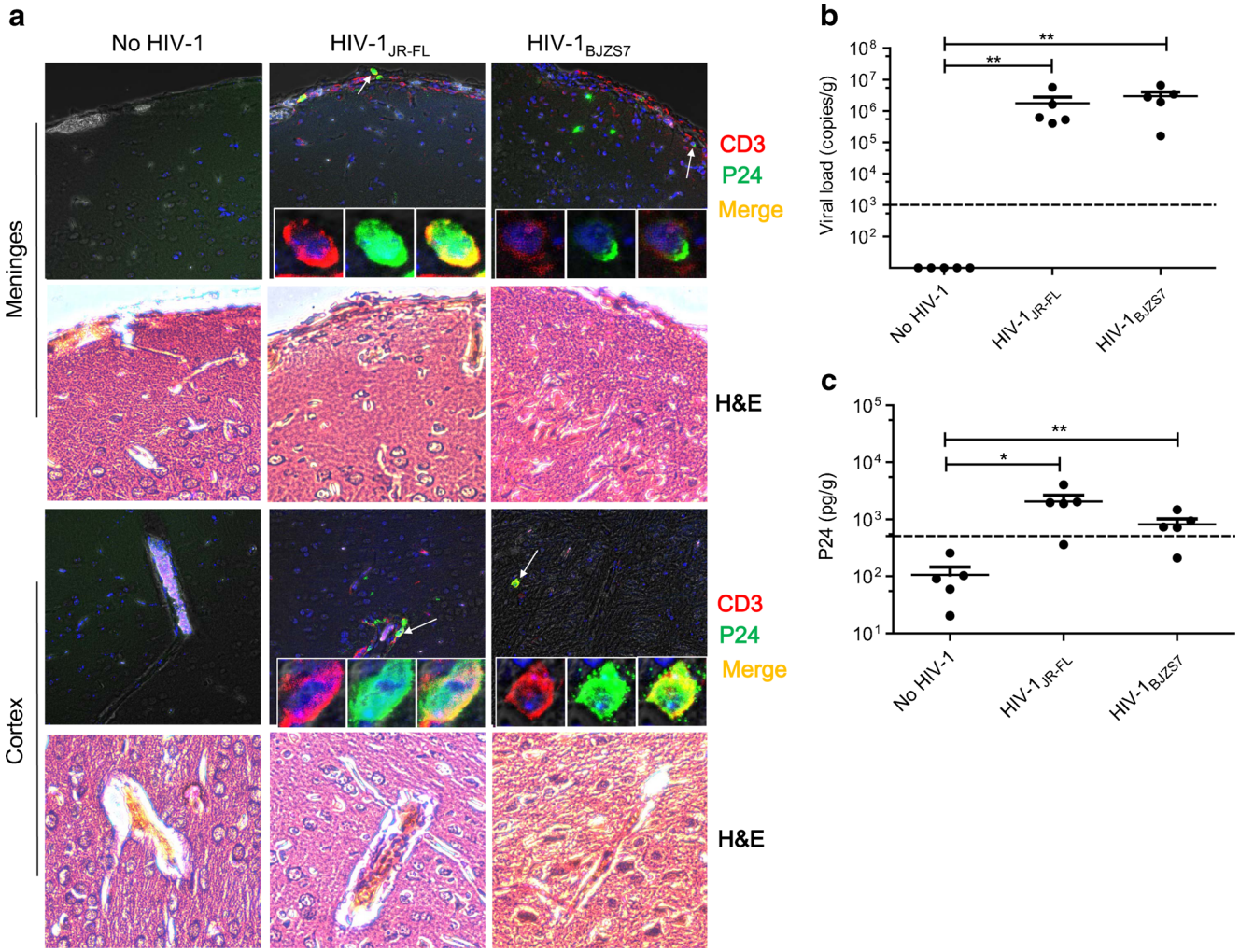

Fig. 5 Brain invasion by infected CD4$^+$ T cells in NSG-HuPBL mice on 14 dpi. **a** Representative sections of meninges (*top*) and cerebral cortex (*bottom*) were analyzed by H&E staining and IHC using antibodies specific to HIV-1 P24 in *green* and to human CD3 in *red* among three groups of mice. The insets are enlarged images of individual cells indicated by corresponding *arrows*. **b** Viral loads were tested in brain homogenates among three groups of NSG-HuPBL mice. **c** P24 antigenemia were determined by ELISA in brain homogenates among three groups of animals. The dash line indicated the detection limit of each assay. *, $p < 0.05$; **, $p < 0.01$

1_{BJZS7} in parallel comparison with the chronic HIV-1_{JR-FL}. Both T/F and chronic viruses were able to infect NSG-HuPBL mice successfully with viral load, P24 antigenemia and P24 positive T cells readily detected in the peripheral blood. Systemic dissemination of both viruses was subsequently found by measuring P24 positive T cells in spleen, liver, kidney, central nerves system and entire mucosal tissues of digestive system of all infected mice on 14 dpi, the Fiebig stage II of acute infection. However, when compared with HIV-1_{JR-FL}, the T/F HIV-1_{BJZS7} appeared to be less pathogenic without causing severe brain neuropathogenesis in terms of microgliosis, astrocytosis and neuron damages, suggesting a possible window of opportunity for HAND intervention. Since the neuron damage was likely associated with levels of microgliosis and P24 antigenemia, early and effective treatment during acute phase of infection might be an attractive strategy to prevent HAND. Our findings, therefore, indicate a useful in vivo model using a T/F HIV-1 to address the issues of acute HIV-1 pathogenesis and early therapeutic interventions.

Various murine models have been developed to study HIV-1 pathogenesis in past 20 years, but to our knowledge, this study for the first time, determined the acute pathogenesis of a primary T/F HIV-1 in humanized NSG-HuPBL mice. Chimeric viruses (e.g. EcoHIV and HIV/VSV) could bypass host restriction of HIV-1 entry, but these models have limitations in target cell tropism, viral transmission and envelope-mediated pathogenesis commonly seen in humans (Hadas et al. 2007; Potash et al. 2005; Roshorm et al. 2009). Therefore, other murine models have been generated using engraftment of functional human immune system to support HIV-1 infection. Because of xeno-reactivity of human T cells in hu-PBL-SCID mice or insufficient human T cell population in SCID-hu Thy/Liv mice, recent studies have focused on NSG and BRG mice that allow a relatively stable functional

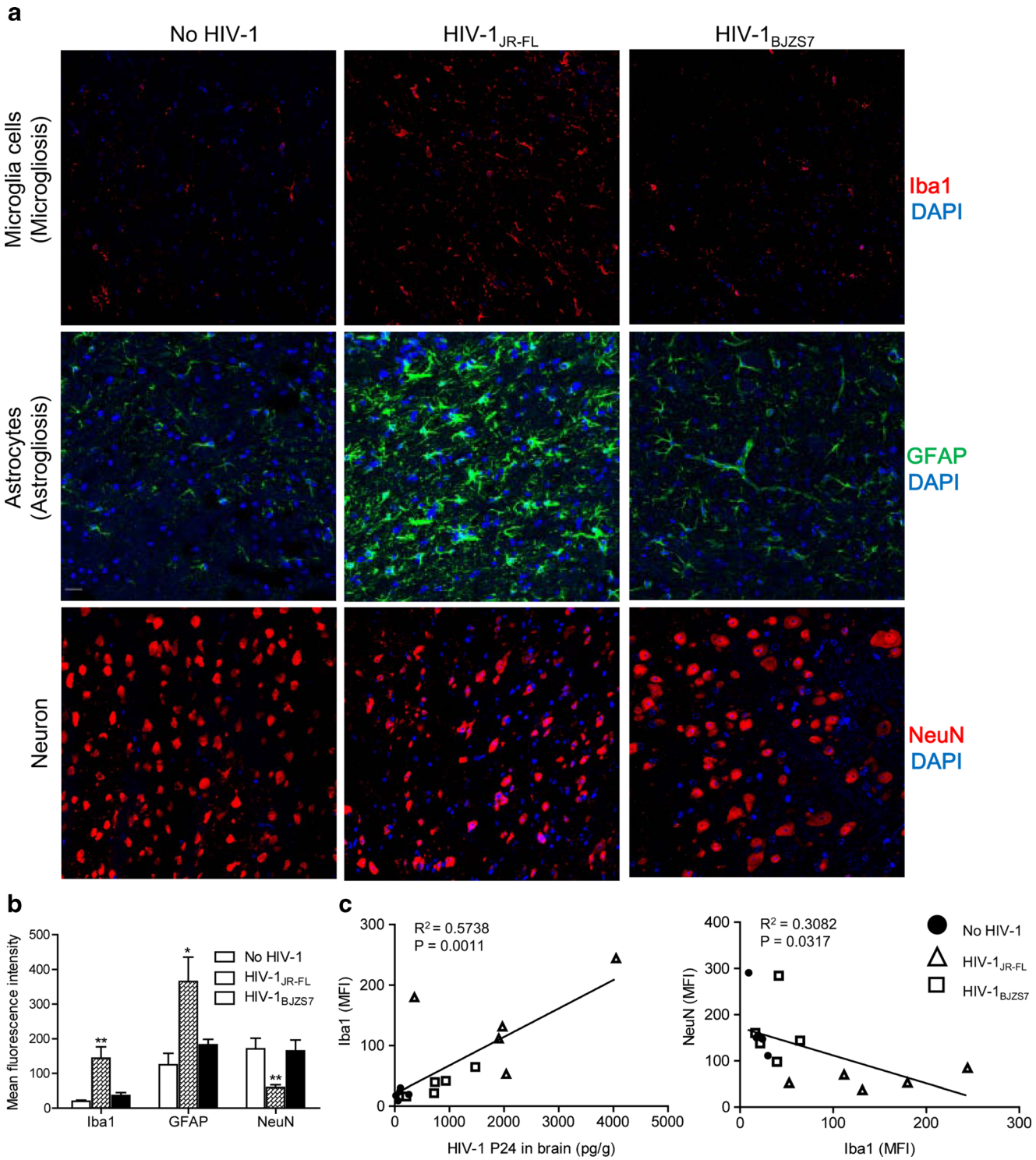

Fig. 6 Neuropathogenesis of HIV-1_{BJZS7} infection in brains of NSG-HuPBL mice. **a** Infection-induced neuropathogenesis was assessed by the expression of Iba-1 and GFAP for activated microglia and activated astrocytes, respectively, as well as NeuN for neuronal damage. **b** Mean fluorescence intensity (MFI) was scored using the NIH Image J software. Five brain sections in each experiment were subjected to quantitative analysis. *, $p < 0.05$; **, $p < 0.01$. **c** Correlation analysis was done by using the GraphPad Prism 5.01 program

human immune system (Baenziger et al. 2006; Watanabe et al. 2007; Zhang et al. 2010). For example, the human T cells can last 43–65 weeks in NSG mice (Singh et al. 2012). NSG mice are considered to be superior to NOD-scid mice in both their peripheral blood reconstitution with multiple classes of human leukocytes and their susceptibility to intravaginal HIV-1 exposure (Stoddart et al. 2011). Although murine models do not reflect the human body completely, they have been used to

answer questions relevant to HIV-1 pathogenesis, latency, protein function as well as the efficacy of neutralizing antibody or drugs (Dash et al. 2012; Gorantla et al. 2010; Gorantla et al. 2012; Long and Stoddart 2012). Here, we show that immunodeficient NOD.Cg-Prkdc scid Il2rgtm1Wjl/SzJ mice, the NSG-HuPBL model of this study, are sufficient to populate human T cells throughout all organ/tissue compartments tested. This finding indicated that in vivo environments in NSG-HuPBL mice likely allowed proper human T cell population, recruitment and tissue homing. Critically, before this study, it remained unknown if a T/F HIV-1 could invade many organ/tissues during the acute phase of infection in NSG-HuPBL mice. This is a critical issue for HIV-1 pathogenesis, prevention and therapy because the T/F virus represents a single viral variant naturally occurring during approximately 80 % of heterosexual transmission events (Joseph et al. 2015; Keele et al. 2008). Our results now confirm that the T/F HIV-1_{BJZS7}-infected T cells were readily detected all major organ/tissue compartments tested besides measurable viral load and P24 antigenemia during the acute phase of infection, which likely reconstitutes the Fiebig stage II of HIV-1 infection (McMichael et al. 2010). Therefore, our findings corroborate that the NSG-HuPBL model is useful for at least the investigation of some acute events of T/F viral pathogenesis.

Direct comparison between the T/F HIV-1_{BJZS7} and the chronic HIV-1_{JR-FL} revealed distinct pathogenic effects in NSG-HuPBL mice. Although we used an equal dose of 10 ng p24 HIV-1 for animal infection, the actual $TCID_{50}$ value of HIV-1_{BJZS7} (646) was higher than that of HIV-1_{JR-FL} strain (466). Since the peak viral loads between two groups were indistinguishable, we speculated that the initial burst replication was similar for both viruses. Subsequently, despite a higher $TCID_{50}$ inoculum, HIV-1_{BJZS7} infection displayed less significant loss of peripheral CD4 T cells, lower antigenemia, and evidently less P24 positive T cells in blood, lung, spleen and submucosal lamino propria on 14 dpi. Furthermore, HIV-1_{BJZS7}-infected mice have yet developed extensive microgliosis, astrocytosis and neuron damages on 14 dpi. The underlying mechanisms remain unknown for these observed differences. Previous studies indicate that due to the blood-brain barrier (BBB) cell free HIV-1 is usually difficult to migrate through brain microvascular endothelial cells, which compose BBB. The virus, however, may engage cell surface heparan and chondroitin sulfate proteoglycans or immune mediators (e.g. TNF-α, IFN-α) to open a paracellular route for brain entry (Bobardt et al. 2004; Fiala et al. 1997; Sas et al. 2009). Moreover, HIV-1 infected blood-borne monocytes/macrophages that repopulate the meninges and perivascular spaces may serve as an efficient way of brain entry in humanized mice (Gorantla et al. 2010). Here, we show that both HIV-1_{BJZS7-} and HIV-1_{JR-FL}-infected $CD4^+$ T cells can rapidly cross BBB as early as the acute Fiebig stage II. Since these infected $CD4^+$ T cells showed strong P24 positive signals, they might still produce live virions after they entered the cerebral cortex. Moreover, we showed that the microgliosis and neuron damages were closely associated with the extent of P24 antgenemia in brain, suggesting the quantity of virus and viral proteins produced might determine the pathogenic consequences including HAND (Dash et al. 2011). This notion is in consistence with previous studies that virus, Tat and gp120 may directly contribute to HAND (Paris et al. 2015; Podhaizer et al. 2012; Zou et al. 2007). Because gp120 glycoproteins can be taken up by brain microvessels and transported across the BBB (Banks et al. 2005), it is possible that higher brain P24 antgenemia in HIV-1_{JR-FL}-infected mice contribute to severer neuron damages as compared with HIV-1_{BJZS7}-infected animals. However we cannot exclude the possibility that HIV-1 strain-specific differences in Tat and gp120 may also determine the neurotoxicity (Podhaizer et al. 2012). To this end, more T/F viruses should be tested in future studies. It should be noted that our NSG-HuPBL mice support persistent human T cell but not peripheral monocyte/macrophage populations. On one hand, it provided a cleaner model to study the role of human T cells during acute HIV-1 brain infection. On the other hand, the role of human monocyte/macrophages in acute brain infection could not be addressed in this study. Since $CD14^+/CD16^+$ macrophage is a potential reservoir of HIV-1 infection in central nervous system (Fischer-Smith et al. 2001), our NSG-HuPBL model should be further improved for human monocyte/macrophage populations by CD34-positive hematopoietic stem cell transplantation and vector-mediated delivery of human cytokines (Huang et al. 2014; Long and Stoddart 2012; Singh et al. 2012). Nevertheless, although the onset of neural injury may date to initial HIV-1 invasion (Ragin et al. 2015), there might still be a window of opportunity for early treatment as HAND prevention especially among T/F cases bearing the neurological phenotype of HIV-1_{BJZS7}.

Acknowledgments The authors would like to thank Hong Kong Council for the AIDS Trust Fund (MSS 227R) for financial support on neuroAIDS research. We also thank Hong Kong Research Grant Council HKU5/CRF/13G to study T cell mechanism and China's 12th 5-year National Science and Technology Mega Project 2013ZX10001005002001 as well as the University Development Fund of the University of Hong Kong and Li Ka Shing Faculty of Medicine Matching Fund to HKU AIDS Institute.

Compliance with Ethical Standards

Conflicts of Interest The authors of this manuscript do not report conflict of interest.

References

Baenziger S et al. (2006) Disseminated and sustained HIV infection in CD34+ cord blood cell-transplanted Rag2−/−gamma c−/− mice. Proc Natl Acad Sci U S A 103:15951–15956. doi:10.1073/pnas.0604493103

Balazs AB, Chen J, Hong CM, Rao DS, Yang L, Baltimore D (2012) Antibody-based protection against hiv infection by vectored immunoprophylaxis. Nature 481:81–84. doi:10.1038/nature10660

Balazs AB et al. (2014) Vectored immunoprophylaxis protects humanized mice from mucosal HIV transmission. Nat Med 20:296–300. doi:10.1038/nm.3471

Banks WA, Kumar VB, Franko MW, Bess JW Jr, Arthur LO (2005) Evidence that the species barrier of human immunodeficiency virus-1 does not extend to uptake by the blood–brain barrier: comparison of mouse and human brain microvessels. Life Sci 77:2361–2368. doi:10.1016/j.lfs.2004.11.041

Bobardt MD et al. (2004) Contribution of proteoglycans to human immunodeficiency virus type 1 brain invasion. J Virol 78:6567–6584. doi:10.1128/JVI.78.12.6567-6584.2004

Budka H et al. (1991) HIV-associated disease of the nervous system: review of nomenclature and proposal for neuropathology-based terminology. Brain Pathol 1:143–152. doi:10.1111/j.1750-3639.1991.tb00653.x

Chen Z, Zhou P, Ho DD, Landau NR, Marx PA (1997) Genetically divergent strains of simian immunodeficiency virus use CCR5 as a coreceptor for entry. J Virol 71:2705–2714

Chen Y et al. (2015) Comprehensive characterization of the transmitted/founder env genes from a single MSM cohort in China. J Acquir Immune Defic Syndr 69:403–412 doi:10.1097/QAI.0000000000000649

Dash PK et al. (2011) Loss of neuronal integrity during progressive HIV-1 infection of humanized mice. J Neurosci 31:3148–3157. doi:10.1523/JNEUROSCI.5473-10.2011

Dash PK et al. (2012) Long-acting nanoformulated antiretroviral therapy elicits potent antiretroviral and neuroprotective responses in HIV-1-infected humanized mice. AIDS 26:2135–2144. doi:10.1097/QAD.0b013e328357f5ad

Fiala M et al. (1997) TNF-alpha opens a paracellular route for HIV-1 invasion across the blood-brain barrier. Mol Med 3:553–564

Fischer-Smith T et al. (2001) CNS invasion by CD14+/CD16+ peripheral blood-derived monocytes in HIV dementia: perivascular accumulation and reservoir of HIV infection. J Neurovirol 7:528–541. doi:10.1080/135502801753248114

Gorantla S et al. (2007) Copolymer-1 induces adaptive immune anti-inflammatory glial and neuroprotective responses in a murine model of HIV-1 encephalitis. J Immunol 179:4345–4356

Gorantla S et al. (2010) Links between progressive hiv-1 infection of humanized mice and viral neuropathogenesis. Am J Pathol 177:2938–2949. doi:10.2353/ajpath.2010.100536

Gorantla S, Poluektova L, Gendelman HE (2012) Rodent models for hiv-associated neurocognitive disorders. Trends Neurosci 35:197–208. doi:10.1016/j.tins.2011.12.006

Hadas E, Borjabad A, Chao W, Saini M, Ichiyama K, Potash MJ, Volsky DJ (2007) Testing antiretroviral drug efficacy in conventional mice infected with chimeric HIV-1. AIDS 21:905–909. doi:10.1097/Qad.0b013e3281574549

Harbison C et al. (2014) Giant cell encephalitis and microglial infection with mucosally transmitted simian-human immunodeficiency virus SHIVSF162P3N in rhesus macaques. J Neurovirol 20:62–72. doi:10.1007/s13365-013-0229-z

Huang J, Li X, Coelho-dos-Reis JG, Wilson JM, Tsuji M (2014) An AAV vector-mediated gene delivery approach facilitates reconstitution of functional human CD8+ T cells in mice. PLoS One 9:e88205. doi:10.1371/journal.pone.0088205

Joseph SB, Swanstrom R, Kashuba AD, Cohen MS (2015) Bottlenecks in HIV-1 transmission: insights from the study of founder viruses. Nat Rev Microbiol 13:414–425. doi:10.1038/nrmicro3471

Kang Y et al. (2012) CCR5 antagonist TD-0680 uses a novel mechanism for enhanced potency against HIV-1 entry, cell-mediated infection, and a resistant variant. Journal Biol Chem 287:16499–16509. doi:10.1074/jbc.M112.354084

Keele BF et al. (2008) Identification and characterisation of transmitted and early founder virus envelopes in primary HIV-1 infection. Proc Natl Acad Sci U S A 105:7552–7557. doi:10.1073/pnas.0802203105

Kumar P et al. (2008) T cell-specific siRNA delivery suppresses HIV-1 infection in humanized mice. Cell 134:577–586. doi:10.1016/j.cell.2008.06.034

Liu J, Gong N, Huang X, Reynolds AD, Mosley RL, Gendelman HE (2009) Neuromodulatory activities of CD4 + CD25+ regulatory T cells in a murine model of HIV-1-associated neurodegeneration. J Immunol 182:3855–3865. doi:10.4049/jimmunol.0803330

Long BR, Stoddart CA (2012) Alpha interferon and HIV infection cause activation of human T cells in NSG-BLT mice. J Virol 86:3327–3336. doi:10.1128/JVI.06676-11

Maartens G, Celum C, Lewin SR (2014a) HIV infection: epidemiology, pathogenesis, treatment, and prevention. Lancet 384:258–271. doi:10.1016/S0140-6736(14)60164-1

Matinella A et al. (2015) Neurological complications of HIV infection in pre-HAART and HAART era: a retrospective study. J Neurol 262:1317–1327. doi:10.1007/s00415-015-7713-8

McMichael AJ, Borrow P, Tomaras GD, Goonetilleke N, Haynes BF (2010) The immune response during acute HIV-1 infection: clues for vaccine development. Nat Rev Immunol 10:11–23. doi:10.1038/nri2674

Minagar A, Shapshak P, Fujimura R, Ownby R, Heyes M, Eisdorfer C (2002) The role of macrophage/microglia and astrocytes in the pathogenesis of three neurologic disorders: HIV-associated dementia, Alzheimer disease, and multiple sclerosis. J Neurol Sci 202:13–23

Nakata H et al. (2005) Potent anti-R5 human immunodeficiency virus type 1 effects of a CCR5 antagonist, AK602/ONO4128/GW873140, in a novel human peripheral blood mononuclear cell nonobese diabetic-SCID, interleukin-2 receptor gamma-chain-knocked-out AIDS mouse model J Virol 79:2087–2096 doi:10.1128/JVI.79.4.2087-2096.2005

Paris JJ, Singh HD, Carey AN, McLaughlin JP (2015) Exposure to HIV-1 Tat in brain impairs sensorimotor gating and activates microglia in limbic and extralimbic brain regions of male mice. Behav Brain Res 291:209–218. doi:10.1016/j.bbr.2015.05.021

Peluso MJ et al. (2013) Cerebrospinal fluid and neuroimaging biomarker abnormalities suggest early neurological injury in a subset of individuals during primary HIV infection. J Infect Dis 207:1703–1712. doi:10.1093/infdis/jit088

Persidsky Y et al. (1996) Human immunodeficiency virus encephalitis in SCID mice. Am J Pathol 149:1027–1053

Podhaizer EM, Zou S, Fitting S, Samano KL, El-Hage N, Knapp PE, Hauser KF (2012) Morphine and gp120 toxic interactions in striatal neurons are dependent on HIV-1 strain. J NeuroImmune Pharmacol 7:877–891. doi:10.1007/s11481-011-9326-z

Potash MJ et al. (2005) A mouse model for study of systemic HIV-1 infection, antiviral immune responses, and neuroinvasiveness. Proc Natl Acad Sci U S A 102:3760–3765. doi:10.1073/pnas.0500649102

Ragin AB et al. (2015) Brain alterations within the first 100 days of HIV infection. Ann Clin Transl Neurol 2:12–21. doi:10.1002/acn3.136

Roshorm Y et al. (2009) Novel HIV-1 clade B candidate vaccines designed for HLA-B*5101(+) patients protected mice against chimaeric ecotropic HIV-1 challenge. Eur J Immunol 39:1831–1840. doi:10.1002/eji.200939309

Rumbaugh JA, Tyor W (2015) HIV-associated neurocognitive disorders: five new things. Neurol Clin Pract 5:224–231. doi:10.1212/CPJ.0000000000000117

Sailasuta N et al. (2012) Change in brain magnetic resonance spectroscopy after treatment during acute HIV infection. PLoS One 7:e49272. doi:10.1371/journal.pone.0049272

Sas AR, Bimonte-Nelson H, Smothers CT, Woodward J, Tyor WR (2009) Interferon-alpha causes neuronal dysfunction in encephalitis. J Neurosci 29:3948–3955. doi:10.1523/JNEUROSCI.5595-08.2009

Singh M et al. (2012) An improved protocol for efficient engraftment in NOD/LTSZ-SCIDIL-2Rgammanull mice allows HIV replication and development of anti-HIV immune responses. PLoS One 7: e38491. doi:10.1371/journal.pone.0038491

Stoddart CA et al. (2011) Superior human leukocyte reconstitution and susceptibility to vaginal HIV transmission in humanized NOD-scid IL-2Rgamma(−/−) (NSG) BLT mice. Virology 417:154–160. doi: 10.1016/j.virol.2011.05.013

Tyor WR, Power C, Gendelman HE, Markham RB (1993) A model of human-immunodeficiency-virus encephalitis in scid mice. Proc Natl Acad Sci U S A 90:8658–8662. doi:10.1073/pnas.90.18.8658

Valcour V et al. (2012) Central nervous system viral invasion and inflammation during acute HIV infection. J Infect Dis 206:275–282. doi: 10.1093/infdis/jis326

Watanabe S et al. (2007) Hematopoietic stem cell-engrafted NOD/SCID/IL2Rgamma null mice develop human lymphoid systems and induce long-lasting HIV-1 infection with specific humoral immune responses. Blood 109:212–218. doi:10.1182/blood-2006-04-017681

Watkins CC, Treisman GJ (2015) Cognitive impairment in patients with AIDS - prevalence and severity. Hiv/Aids 7:35–47. doi:10.2147/HIV.S39665

Zhang L, Meissner E, Chen J, Su L (2010) Current humanized mouse models for studying human immunology and HIV-1 immuno-pathogenesis. Sci China Life Sci 53:195–203. doi:10.1007/s11427-010-0059-7

Zhuang K et al. (2014) Emergence of CD4 independence envelopes and astrocyte infection in R5 simian-human immunodeficiency virus model of encephalitis. J Virol 88:8407–8420. doi:10.1128/Jvi.01237-14

Zou W, Kim BO, Zhou BY, Liu Y, Messing A, He JJ (2007) Protection against human immunodeficiency virus type 1 Tat neurotoxicity by *Ginkgo biloba* extract EGb 761 involving glial fibrillary acidic protein. Am J Pathol 171:1923–1935. doi:10.2353/ajpath.2007.070333